Methane Concentration at Heading Faces With Auxiliary Ventilation

Shinji Tomita, Kenichi Uchino, and Masahiro Inoue
Kyushu University
Fukuoka, Japan

ABSTRACT

Three-dimensional airflow velocities at a heading face by a forcing or exhausting auxiliary ventilation system were measured in an actual size model gallery and in an actual mine. There were several stagnated regions near the roof corner, which might have danger of methane accumulation. Airflow velocities by an exhausting system were much smaller than that by a forcing system.

The airflow and methane concentrations by a forcing, exhausting, or combined system were examined using a visualization technique by laser light in a reduced scale model. Water was used instead of air and very fine bubbles generated by electrolysis were employed as tracer. The behavior of the bubbles in water is similar to that of methane in the air.

Accumulation of bubbles was observed at the roof corner of the face which corresponds to the region that the airflow stagnation was observed in the previous actual size model experiment. The optimal airflow rate through a forcing and exhaust duct and duct end locations to reduce hazard of methane accumulation were investigated for the combined system of ventilation.

Experiments on methane accumulation using real methane in the air were also conducted in other reduced scale model.

KEYWORDS

Heading Face, Auxiliary Ventilation, Methane Gas, Visualization, and Electrolysis of Water.

INTRODUCTION

Auxiliary ventilation at heading faces is very important in coal mines for controlling gases, dust and heat which are emitted at increasing rates today as a result of enhanced driving rates and deepening working levels. There are several researches about the airflow velocities and directions at heading faces (Wesely, 1984; Shuttleworth, 1963; Uchino and Inoue, 1997).

However, because of the complexity of airflow in the face area it is not easy to find the ventilation method that is technologically optimum for heading faces of various conditions. From this point of view the airflow and methane concentration at heading faces with auxiliary ventilation were investigated by three methods.

Firstly, airflow velocities at a heading face were measured in an actual size model gallery and an actual mine. Secondly, methane accumulations were investigated using a visualization technique by laser light in a reduced scale model. Water was used instead of air and bubbles generated by electrolysis were employed as tracer. Thirdly, methane accumulation using real methane in the air was investigated in another reduced scale model.

EXPERIMENT BY AN ACTUAL SIZE MODEL GALLERY

Velocity vectors of airflow in a heading face were measured in an actual size model gallery 2.8 m in width and 2.4 m in height, as shown in Fig.1. The duct 48 cm in diameter was set on the center or corner of the roof side of gallery and the airflow by forcing or exhausting system was examined. The distances between the face and the duct end were 5, 7, and 10 m in forcing ventilation, and were 3 and 5 m in exhausting ventilation. However, discussions will be made mainly with the distance of 7 m in forcing ventilation and 3 m in exhausting ventilation, because not much difference was

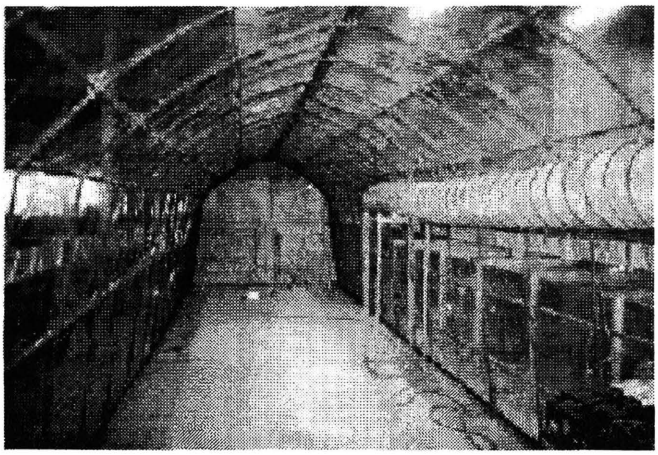

Figure 1. Actual size model gallery.

Figures 2 (a) and (b) show the airflow vectors on a vertical section through the roadway axis and on a vertical section 0.2 m from the sidewall respectively at the heading face with forcing ventilation when the duct is set on the center of the roof. An air jet from the duct advances towards the face spreading out gradually. After reaching the face, the airflow descends along the face and returns. A part of the air returning from the face is entrained again into the air jet discharged from the duct.

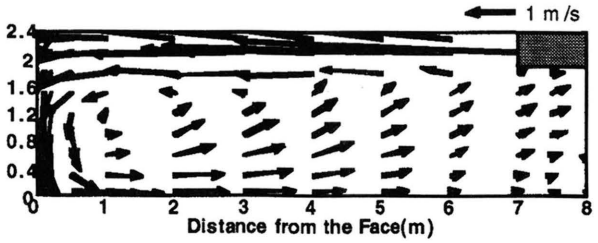

(a) Vertical section through the roadway axis.

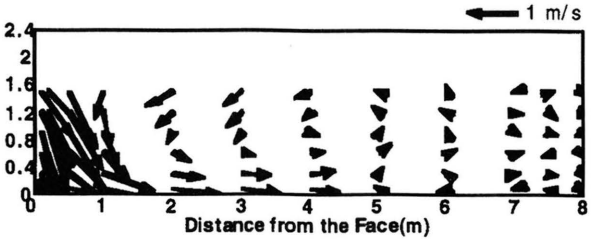

(b) Vertical section 0.2 m from the sidewall.

Figure 2. Airflow vectors at the heading with forcing ventilation in an actual size model (duct position: roof center).

Figures 3 (a) and (b) show the airflow vectors on a vertical section just beside the duct and on a vertical section 0.2 m from the sidewall respectively at the heading face with forcing ventilation when the duct is set on the corner of the roof. Airflow velocity towards the face is high but return flow is hardly seen in Figure (a). Figure (b) shows that return flow travels almost parallel to the floor without being affected by the jet from the duct end.

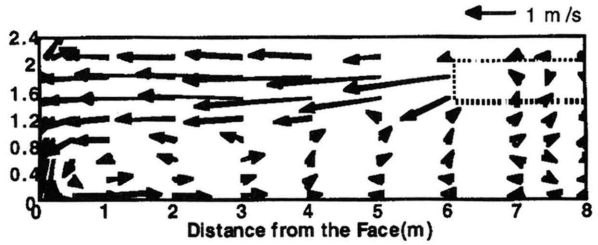

(a) Vertical section just next to the duct.

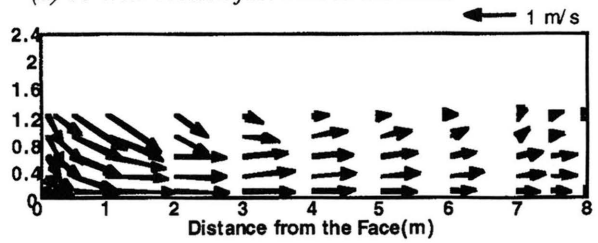

(b) Vertical section 0.2 m from sidewall.

Figure 3. Airflow vectors at the heading with forcing ventilation in an actual size model (Duct position: roof corner).

Figure 4 shows the difference of airflow on a horizontal section 0.4 m below the roof when the duct end is located on the center of the roof (Figure 3(a)) and on the corner of the roof (Figure 3(b)). Airflow velocities at the faces are high in these figures, but there are some stagnated regions at the corner of the roof and the outby area of the duct end. Airflow velocities from the duct are maintained at relatively high speed in wider area when the forcing duct end is located on the corner of the roof.

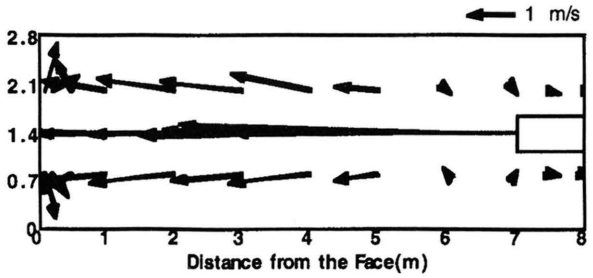

(a) Roof center.

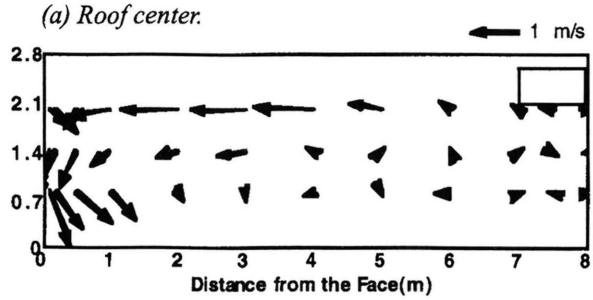

(b) Roof corner.

Figure 4. Airflow vectors in a heading 0.4 m from below the model roof in a forcing ventilation system.

Figure 5 shows the airflow vectors at the heading face with exhausting ventilation when the duct is set on the center of the roof. Figure 5(a) shows the airflow vectors on a vertical section through the roadway axis and Figure 5(b) those on a horizontal section 1.6 m from the floor, respectively. Note that an air velocity corresponds to a unit length of arrow in these figures and is one tenth of the velocities in the previous figures. In general, airflow velocities by the exhausting system are much smaller, as compared to that by the forcing system. A region ventilated directly by fresh air, which comes from behind the exhaust duct end, is limited within about 1.5 m ahead of the duct end. Airflow in this region is stable. Very slow secondary airflow is observed near the face. The secondary airflow is caused by the airflow to the exhausting duct end directly.

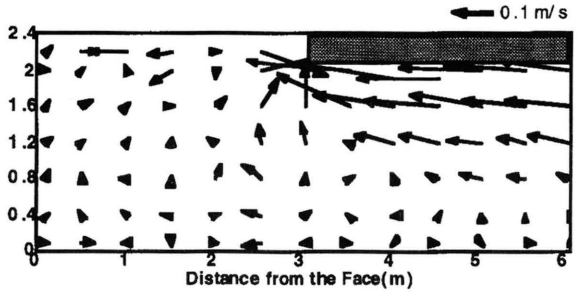

(a) Vertical section through the roadway axis.

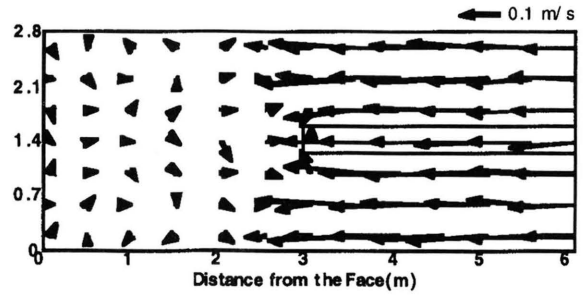

(b) Horizontal section 1.6 m from the floor.

Figure 5. Airflow vectors in a heading under exhausting ventilation system.

Figure 6 shows the airflow vectors at the heading face with exhausting ventilation when the duct is set on the corner of the roof. Figure 6(a) shows the airflow vectors on a vertical section just beside the duct and Figure 6(b) shows those on a horizontal section 1.6 m from the floor. Behind the duct end, a stable airflow whose velocity is over 0.1 m/s is seen near the floor and opposite side of duct position. Secondary airflow near the face is also very slow.

In-situ measurements were performed at Hishikari gold mine, and the results show satisfactory coincidence in airflow distribution with the model experiment.

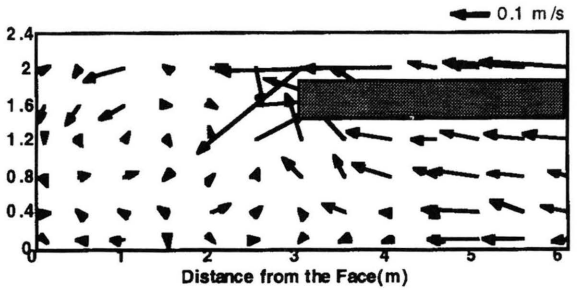

(a) Vertical section through the roadway axis.

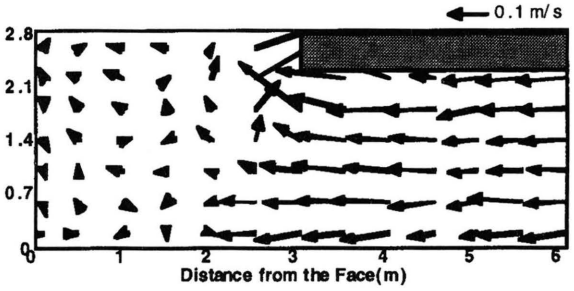

(b) Horizontal section 1.6 m from the floor.

Figure 6. Airflow vectors at the heading with exhausting ventilation system (duct position: roof corner).

FLOW VISUALIZATION USING BUBBLES

It is always difficult to investigate methane accumulation in a heading underground or in an actual size model gallery. Therefore, a combination of laser light and minute bubbles is used to simulate and visualize the methane accumulation at the heading face in a reduced scale model as shown in Figure 7.

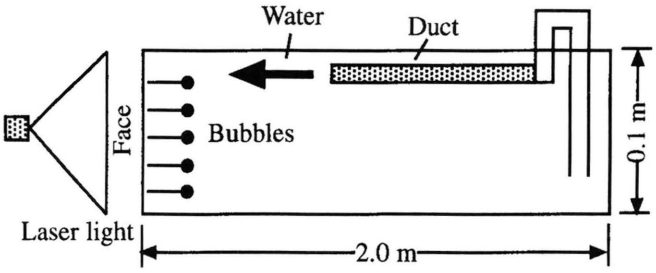

Figure 7. Model gallery used in the experiment.

It is a one-thirtieth scale model with rectangular cross section 20 cm width and 10 cm height. Water was used instead of air and minute bubbles generated by electrolysis as tracer. Bubbles were generated on the face. Brighter regions in visualized pictures mean higher concentration of bubbles. Flow rate, the distance between the duct end and

the face, the shape of face and roof with forcing, exhausting, or combined ventilation system were examined. The diameters of the forcing and exhausting duct were 3 cm and 2 cm respectively. Each duct was set on the each corner of the roof.

Figure 8 shows the distribution of bubbles when there is no flow in the model. Bubbles generated at the heading face move upward along the face first, then move to outby side (right side of the figure) along the roof. A layer of bubbles was formed below the roof just as methane does. The behavior of bubbles in water is quite similar to that of methane in the air.

Figure 8. Distribution of bubbles generated by electrolysis in the heading (no flow).

Figure 9 shows the distribution of bubbles when the forcing system is utilized. The distance from the face to the forcing duct end is (a) 23.3 cm and (b) 33.3 cm (7, 10 m in actual size). The forcing flow rate is 60 l/min.

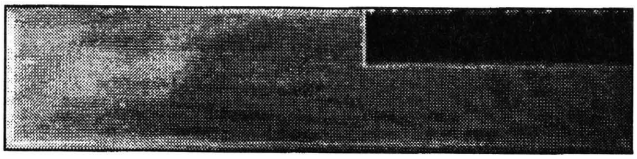

(a) Bubble distribution when distance between face and end of duct is 23.3 cm.

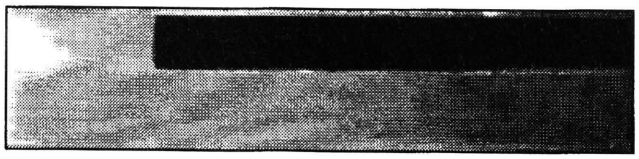

(a) Bubble distribution when distance between face and end of duct is 10 cm.

Figure 9. Bubble distribution in heading using forcing ventilation system.

Throughout the all experiments, the concentration of bubbles was lowest on a vertical section through the duct center and was highest on a vertical section beside the opposite sidewall of the duct. If the forcing jet flow reached to the face, the bubbles mix well with water. The local concentration of bubbles decreased with increase in flow rate. On the other hand the concentration of bubbles becomes higher when the distance from the face and the duct end is too short.

At heading faces in actual mines, the surface of the roof is rough because of supports and cavings, and there are some obstacles such as road heading machines. Figure 10 shows the distribution of bubbles in these cases when the forcing system is utilized. Figure 10(a) shows the influence of the roughness of the surface of the roof. The jet flow becomes more turbulent because of the rough roof and the bubbles are mixed with water well. Figure 10 (b) shows the influence of a caving at the face. The bubbles accumulate in the cavings, where eddy flow is seen. Figure 10(c) shows the influence of a road heading machine placed at the face. In this case, the concentration of bubbles near the face and the roof are higher when the machine is placed at the face although the concentration is lower as a whole when the machine is not placed.

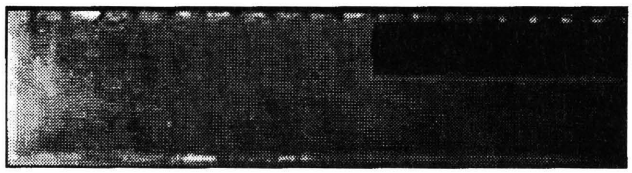

(a) Influence of roof surface roughness.

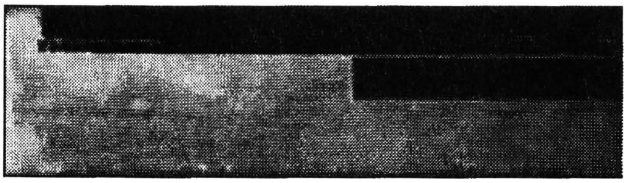

(b) Influencd of caving in the heading.

(c) Influence of a roadheader of machine.

Figure 10. Bubble distribution in the heading using forcing ventilation system under various mining conditions.

Figure 11 shows the distribution of bubbles when the exhausting system is utilized. Figures 11 (a) and 11(b) show the distribution when the distance from the face to the duct end is 10 cm and 16.7 cm (3, 5 m in actual size). As it was shown in Figure 5, a region ventilated directly by the flow, which comes from behind the exhaust duct end, is limited within quite a short distance ahead of the duct end. Consequently the bubbles concentration is very high near the face as shown in Figure 11. The bubbles are not observed behind the duct end.

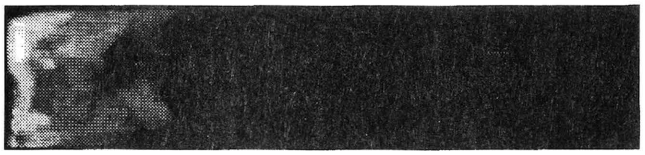

(a) Distance between face and end of duct is 10 cm.

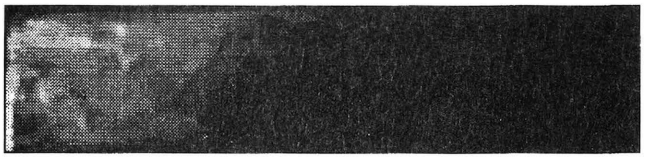

(b) Distance from the face to the duct end is 16.7 cm.

Figure 11. Distribution of bubbles in the heading using exhausting ventilation.

The overlap ventilation system, that is, forcing system combined with exhausting system, will be used considerably in Japanese coalmines to control the dust and methane gas at the same time. However, there is almost no published work about the optimization of the overlap system.

Figure 12 shows the distribution of bubbles when the forcing overlap system is utilized. The distances from the face to the forcing duct end are (a) 10 cm, (b) 16.7 cm, and (c) 23.3 cm (3, 5, and 7 m in actual size). Flow velocities are 1.4 m/s (flow quantity is 60 l/min) in the forcing duct and 5.3 m/s (flow quantity is 100 l/min) in the exhausting duct. The figure (b) shows the best performance to discharge the bubbles from the face compared to other cases. The figure (d) shows the distribution when all the conditions are same with that of (b) except the flow velocity of the exhausting duct is decreased from 5.3 m/s to 4.2 m/s (flow quantity is 80 l/min). In this case, the performance to discharge the bubbles decreased apparently.

It is not so easy to recognize clearly the difference in concentration of bubbles from the figures as shown Figure 9, etc. However, these differences can be easily represented if pictures are enhanced using a computer. Figure 13 shows the same distribution of bubbles with Figure 9. The minimum brightness in the figure is set to be 0 (painted black) and the maximum one is set to be 255 (painted white). It is easy to recognize that the brightness near the face is higher in the Figure 13(b).

MEASUREMENT OF METHANE CONCENTRATION

The distribution of methane concentration at the heading face with forcing ventilation was investigated in a reduced scale model gallery. The gallery is a one-fifteenth scale model with rectangular cross section 40 cm width and 20 cm height. Methane gas was emitted from the face. The forcing duct was set on the center of the roof. The distance from the face to the duct end was 50 cm (7.5 m in actual size). The diameter of the duct was 6 cm.

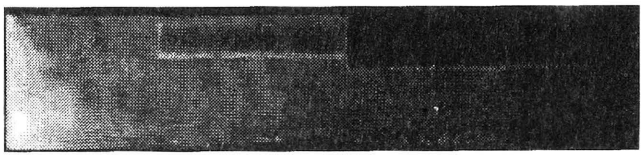

(a) Total exhausting air quantity: 100 l/min with distance between face and duct at 10 cm.

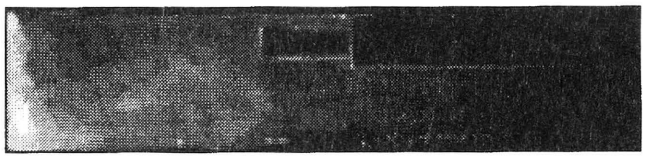

(b) Total exhausting air quantity: 100 l/min with distance between face and duct at 16.7 cm.

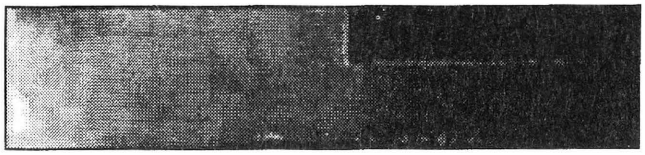

(c) Total exhausting air quantity: 100 l/min with distance between face and duct at 23.3 cm.

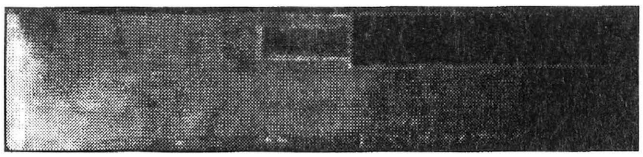

(d) Total exhausting air quantity: 80 l/min with distance between face and duct at 16.7 cm.

Figure 12. Bubble distribution in the heading with overlapping forcing ventilation

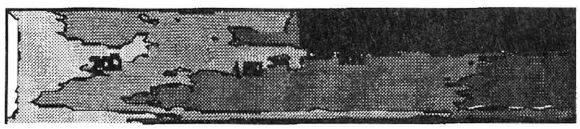

(a) Distance between face and duct: 23.3 cm.

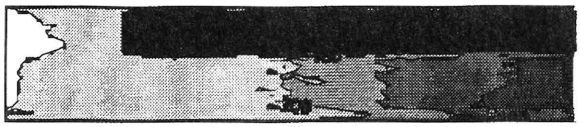

(a) Distance between face and duct: 23.3 cm.

Figure 13. Various computer enhanced brightness contours indicating bubble concentration as shown in Figure 9.

Figure 14 shows the distribution of methane concentration when there is no flow and the flow rate of methane from the face is 5 l/min. Methane emitted from the face moves up along the face first and then moves along the roof. This result coincides with Figure 8. Methane concentration near the floor is almost 0 %.

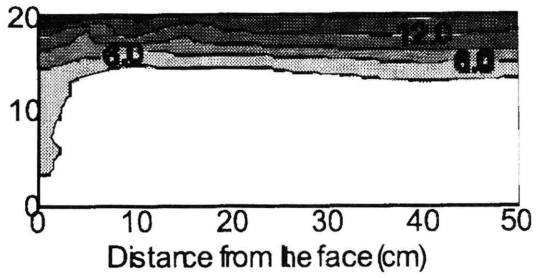

Figure 14. Methane concentration distribution without any airflow.

Figure 15 shows the distribution of methane concentration when forcing velocity is 1 m/s and the flow rate of methane from the face is 5 l/min. Figure 15(a) shows the distribution of methane on a vertical section through the center of the model while Figure 15(b) shows that on a vertical section near the sidewall. The air jet doesn't reach the face under this condition, resulting in high concentration near the face. The methane is difficult to be discharged from the bottom of the face because airflow velocity is very slow and a stagnated region is formed.

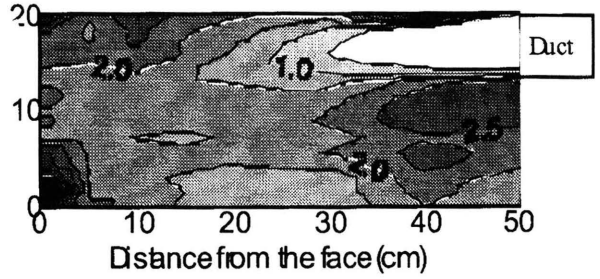

(a) Vertical section through the center of the model.

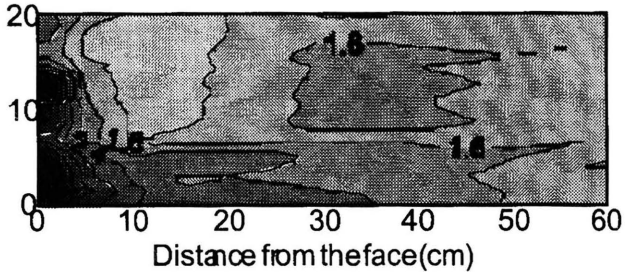

(a) Vertical section near the sidewall.

Figure 15. Methane concentration distribution with an airflow velocity of 1 m/sec.

Figure 16 shows the distribution of methane concentration when forcing velocity is 3 m/s and the flow rate of methane from the face is 5 l/min. Figure 16(a) shows the distribution of methane on a vertical section through the center of the model while Figure 16(b) shows that on a vertical section near the sidewall. Methane is fully diluted with air near the roof. But there is a high concentration region near the floor. Figure 16(b) shows that there is enough return airflow near the roof to prevent methane layering. However, the methane concentration near the floor is high.

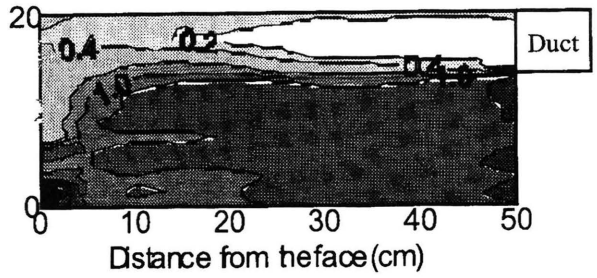

(a) Vertical section through the center of the model.

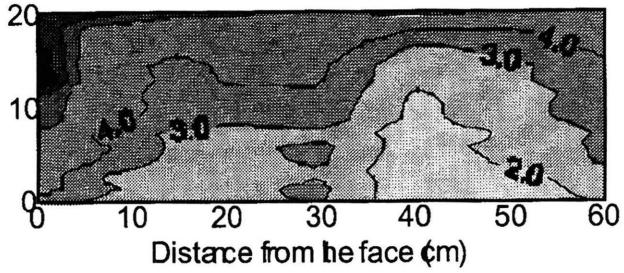

(b) Vertical section near the sidewall.

Figure 16. Methane concentration distribution with an airflow velocity of 3 m/sec.

When the forcing velocity is 5 m/s, CH_4 distribution is similar to that in Figure 16. The distribution of methane concentration seems to depend on whether the forcing jet reaches to face. Although methane is lighter than air, it has also been detected near the floor as well.

CONCLUSION

Airflow velocities and methane concentration in a heading with auxiliary ventilation were investigated by three different methods. Results are summarized as follows:

(1) Fundamental airflow patterns at the face with forcing or exhausting ventilation were obtained.

(2) Methane accumulation at the heading was visualized by using a combination of laser light and minute bubbles. Bubbles were mixed with water well when the surface of the roof was rough. However, bubbles tend to accumulate in large depressions. When a road header machine was placed in the face, bubbles accumulated near the roof and the face.

When overlap system was utilized, bubbles accumulation was affected not only by the locations of the ventilation duct but also by the flow rates through the ducts.

(3) Experiments on methane accumulation using real methane were conducted. The distribution of methane shows good corelations with bubbles used in the experiments.